ECOCYCLES
ISSN 2416-2140

OPEN ACCESS
Scientific journal of the
European Ecocycles Society

Ecocycles, Vol., 12, No. 1, pp. 38-49 (2026)
DOI: 10.19040/ecocycles.v12i1.645

RESEARCH ARTICLE

Sewage-sludge-based activated carbon as a sustainable adsorbent for near-complete removal of 6PPD-quinone at environmentally relevant levels

Nina Ricci Nicomel[1], Loretta Y. Li[1]*

[1]*Department of Civil Engineering, University of British Columbia, 6250 Applied Science Lane, Vancouver, BC V6T 1Z4, Canada*

**Corresponding author: Prof. Dr. Loretta Li, Email address: lli@civil.ubc.ca*

Abstract – The tyre-derived transformation product 6PPD-quinone (6PPD-q) poses a growing threat to aquatic ecosystems, particularly sensitive salmonid species. However, practical and affordable treatment options remain limited. This study investigated the potential of sewage-sludge-based activated carbon (SBAC) produced via $ZnCl_2$ activation and pyrolysis as a sustainable adsorbent for removing 6PPD-q from contaminated water and advancing circular-economy approaches for sludge valorisation. Fourier-transform infrared spectroscopy revealed the presence of oxygen-containing surface groups on SBAC that can facilitate hydrogen bonding and π–π interactions with 6PPD-q. Batch adsorption experiments were performed to evaluate equilibrium behaviour and thermodynamic properties under controlled conditions. Results showed rapid uptake, achieving >99% removal from an initial concentration of 200 µg/L within 0.5 h at pH 3.5. The Langmuir model best fit the equilibrium data, with R^2 value of 0.95, yielding a maximum adsorption capacity of 583.3 µg/g. Thermodynamic analysis indicated a spontaneous and endothermic process, suggesting chemisorption as the dominant mechanism. The adsorption efficiency remained stable within the temperature range of 7°C–35°C, and sequential treatments maintained high removal performance. The experimental results demonstrate that SBAC is an efficient and low-cost adsorbent for mitigating 6PPD-q contamination in stormwater, offering a sustainable solution for valorising sewage sludge within circular economy frameworks.

Keywords – Tyre-derived contaminant, Sludge valorisation, Adsorption kinetics, Carbonaceous adsorbents, Stormwater, Aquatic life.

Received: December 09, 2025 Accepted: January 18, 2026

1. INTRODUCTION

Non-exhaust particulate (NEP) emissions from road traffic, including tyre, brake and pavement wear, are major contributors to the deterioration of urban stormwater quality and degradation of aquatic and terrestrial ecosystems (Chae et al., 2021; Wang et al., 2022). Tyre wear alone accounts for an estimated global per capita release of 0.81 kg per year (Halle et al., 2021). The increasing complexity of materials used in tyre and brake pad manufacturing, combined with limited transparency in product formulations (Beji et al., 2021), underscores the need for comprehensive studies to mitigate the ecological and human health risks associated with NEP emissions. Moreover, many NEP-derived compounds undergo complex degradation and transformation, generating potentially more toxic by-products (Cao et al., 2022), intensifying environmental concerns.

One such compound is *N*-(1,3-dimethylbutyl)-*N*′-phenyl-*p*-phenylenediamine (6PPD), a synthetic antioxidant that has been intentionally added to rubber formulations since the 1960s to protect tyres from oxidative degradation (Lane et al., 2024). 6PPD functions as an antidegradant by reacting with tropospheric ozone at the tyre surface, thereby preventing ozone-induced cracking and prolonging tyre lifespan (Greer et al., 2023). During this process, 6PPD is oxidised, resulting in the formation of a quinoid transformation product, *N*-(1,3-dimethylbutyl)-*N*′-phenyl-*p*-phenylenediamine (6PPD)-quinone (6PPD-q) (Nicomel and Li, 2023). Although 6PPD has been widely used for decades, the formation of 6PPD-q via ozonation was only identified recently (Tian et al., 2021), revealing a critical gap in the prior understanding of tyre-derived chemical emissions and their environmental fate.

While 6PPD-q is frequently detected in surface waters, its dominant pathway to the hydrosphere remains under investigation. Current evidence indicates that 6PPD is primarily released during tyre wear, subsequently oxidised to 6PPD-q and transported to aquatic systems mainly via stormwater runoff. Tyre and road wear particles are largely associated with the PM_{10} fraction and partly with the $PM_{2.5}$ fraction (Nicomel and Li, 2023). Leaching from disposed or ageing tyres may occur locally but appears to be a secondary pathway and is more readily controlled through waste management practices. Once mobilised into urban runoff, however, 6PPD-q has emerged as a highly toxic tyre-derived contaminant of concern.

6PPD-q has recently been identified as a cause of acute mortality in coho salmon (*Oncorhynchus kisutch*) (Tian et al., 2021) and has been shown to induce developmental, behavioural and cardiotoxic effects in zebrafish larvae (Varshney et al., 2022). Other aquatic species, such as *Oncorhynchus keta*, *Danio rerio*, *Oryzias latipes*, *Daphnia magna* and *Hyalella azteca*, show lower but measurable sensitivity (Hiki et al., 2021; McIntyre et al., 2021). The reported environmental concentrations of 6PPD-q range from 0.08 to 19 µg/L in stormwater and <0.2 to 3.5 µg/L in surface waters (Challis et al., 2021; Johannessen et al., 2022; Tian et al., 2021). Given the low median lethal concentration (LC_{50}) of 0.8 ± 0.2 µg/L for juvenile coho salmon (Tian et al., 2021) and the recently established short-term acute water-quality guideline of 0.01 µg/L (Chalifour et al., 2025), even trace contaminations pose substantial ecological risks. These findings highlight the need for effective stormwater treatment, particularly in high-traffic areas, as the growing adoption of heavier electric vehicles may further intensify tyre wear and 6PPD-q emissions (Johannessen et al., 2022; Liu et al., 2021).

Although research on 6PPD-q is still in its nascent stage, several researchers have investigated potential removal pathways, including ultraviolet-activated peroxymono-sulfate treatment (Yu et al., 2024), adsorption onto metal-organic framework nanosheets (Wu et al., 2025) and microbial degradation for transforming and detoxifying 6PPD-q (Yu et al., 2025). Despite these advances, practical and scalable treatment options for urban stormwater remain limited. To ensure sustainable development and a circular economy, treatment strategies must be both cost-effective and environmentally friendly. Hence, developing efficient and low-impact approaches for removing 6PPD-q from stormwater remains a key area for further investigation.

Adsorption using activated carbon (AC) is widely used as an efficient technology for removing emerging pollutants from water, given its effectiveness even at low contaminant concentrations, suitability for batch and continuous processes and potential for regeneration and reuse (Jeirani et al., 2017). Sewage sludge (SS) is a commonly used precursor for producing AC (Mu'azu et al., 2017) because of its high availability, carbon-rich composition and substantial organic matter content (Luján-Facundo et al., 2020). Notably, SS disposal remains a critical challenge in the global waste sector, with production rates ranging from 35 to 85 g dry matter per capita per day (Werle and Sobek, 2019). In this context, converting waste SS into sewage-sludge-based activated carbon (SBAC) can support sustainable sludge management and provide a valuable material for pollutant control, aligning with circular economy principles. Furthermore, several studies have shown that contaminants commonly found in SS can be effectively stabilised during SBAC production (Li et al., 2019; Mohamed et al., 2023a,b; Montoya-Bautista et al., 2022).

SBAC effectively removes various organic and inorganic contaminants, such as polycyclic aromatic hydrocarbons, phenols and phthalates (Björklund and Li, 2017; Sullivan et al., 2019); nutrients (Yue et al., 2018); pharmaceutical and personal care products (Montoya-Bautista et al., 2022); *p*-benzoquinone (Nicomel et al., 2022b) and metals (Li et al., 2019; Nicomel et al., 2022a). In most cases, $ZnCl_2$ is used as the activating agent because it yields high specific surface areas (>700 m^2/g) and well-developed porosity by selectively removing hydrogen and oxygen from the raw material, thereby minimising tar formation (Li et al., 2019; Zhao et al., 2022).

To the best of our knowledge, no studies have investigated the adsorption of 6PPD-q using either SBAC or AC, particularly at environmentally relevant concentrations (µg/L levels). Research on 6PPD-q removal has primarily focused on oxidation or catalytic degradation at considerably higher concentrations (e.g. 1 mg/L), which does not reflect the conditions typical of urban runoff (Yu et al., 2025, 2024). The use of SBAC for 6PPD-q removal aligns with circular economy principles because it enables the conversion of waste into a value-added material for stormwater treatment. Thus, evaluating the adsorption performance at low 6PPD-q levels is essential for assessing the suitability of SBAC integration into green infrastructure systems (e.g. rain gardens) for mitigating tyre-derived contaminants in urban waters.

Considering these aspects, this study aimed to evaluate the potential of SBAC to effectively reduce 6PPD-q concentrations in stormwater. The hypothesis was that hydrophobic 6PPD-q can be efficiently retained on the porous carbon surface of SBAC through hydrophobic interactions and surface affinity. To explore this, the following objectives were established: (1) estimate the maximum adsorption capacity of SBAC for 6PPD-q and identify a working concentration near saturation; (2) determine the effects of key adsorption parameters, including adsorbent dosage, contact time and temperature; (3) assess the ability of SBAC to achieve the short-term acute water-quality guideline of 0.01 µg/L through sequential adsorption cycles; (4) compare the 6PPD-q removal efficiencies of SBAC and commercial AC; (5)

characterise the surface functional groups of SBAC before and after adsorption to elucidate possible adsorption mechanisms. The practical implication of this study is its contribution to waste-to-resource framework in waste management that support environmental sustainability and align with circular economy principles. The findings can be applied to treat water contaminated with 6-PPD-quinone, and SBAC can also be used to enhance the performance of biofilters to remove not only tyre-derived chemicals but also other hydrophobic organic contaminants present at environmentally relevant levels in stormwater, thereby helping protect aquatic life.

2. MATERIALS AND METHODS

2.1 Materials and chemicals

The standards 6PPD-quinone (100 μg/mL in acetonitrile) and D5-6PPD-quinone (>95% purity) were obtained from HPC Standards GmbH (Germany) and LGC Ltd. (Canada), respectively. Deionised (DI) water from a Synergy® UV Water Purification System (Merck, Darmstadt, Germany) was used to prepare all aqueous solutions. A stock solution of 6PPD-q (1000 μg/L) was prepared and used to obtain a 200 μg/L working solution.

2.2 Preparation of sewage sludge-based activated carbon

SS was collected from a wastewater treatment plant in British Columbia, Canada (location not disclosed). The sludge was dewatered by centrifugation at 3000 rpm for 3 min using a BECKMAN GS-6 centrifuge (Marshall Scientific, Hampton, NH), dried at 105°C for 48 h and ground and sieved to <250 μm. Chemical activation was performed by soaking the precursor in a $ZnCl_2$ solution at a ratio of 1 g SS to 2 mL of solution. The activated sample was oven-dried at 105°C for 24 h, pyrolysed at 500°C for 2 h, homogenised (<250 μm), acid-washed, rinsed with DI water and dried overnight at 105°C. Details of the SBAC production process are provided by Gong (2013) and Mohamed et al. (2022). The physicochemical characteristics of the resulting SBAC are summarised in Table S1 of the Supplementary Information (SI).

2.3 Adsorption of 6PPD-quinone

For the batch adsorption tests, 10 mg of SBAC was mixed with 10 mL of the 6PPD-q working solution in 15-mL glass centrifuge tubes. The suspensions were agitated using an end-over-end rotator at 35 rpm for 24 h at room temperature (20°C ± 2°C). After equilibration, the mixtures were filtered using Whatman® Puradisc 0.7-μm GF/F syringe filters (Merck, Germany). The pH of each sample was recorded before and after adsorption. Filtrates were analysed for 6PPD-q concentrations using liquid chromatography–tandem mass spectrometry (LC–MS/MS; Orbitrap Exploris 240, Thermo Fisher Scientific, Waltham, MA). The removal efficiency and adsorption capacity were calculated using Eqs. S-1 and S-2 provided in the SI.

2.3.1 Maximum adsorption capacity (q_{max})

To determine q_{max}, batch adsorption experiments were conducted with initial 6PPD-q concentrations of 20–500 μg/L. The equilibrium data were fitted using both the Langmuir and Freundlich isotherm models to describe the adsorption behaviour. Based on these results, the working solution concentration for subsequent experiments was selected close to the saturation region to ensure measurable removal without complete surface saturation.

2.3.2 Effect of adsorbent dosage

The effect of adsorbent dosage on 6PPD-q removal was assessed to identify the minimum amount of SBAC needed for effective and practical adsorption. Dosage levels of 1, 2 and 3 g/L were tested.

2.3.3 Effect of contact time

The influence of contact time was assessed at 0.5 and 24 h using the optimum SBAC dosage at room temperature (20°C ± 2°C). These intervals were chosen to verify whether 6PPD-q exhibits the rapid uptake previously observed for other contaminants using SBAC (Nicomel et al., 2022b).

2.3.4 Effect of temperature

Batch adsorption tests were performed at 7°C, 20°C and 35°C to investigate the effect of temperature on 6PPD-q adsorption. This range reflects typical environmental conditions, and it was selected to determine how temperature influences the interaction between SBAC and 6PPD-q. The thermodynamic analyses are summarised in Section S-2 in the SI.

2.3.5 Sequential adsorption tests

The ability of SBAC to reduce 6PPD-q concentrations to below the short-term acute water-quality guideline of 0.01 μg/L (Chalifour et al., 2025) was evaluated using repeated adsorption cycles. In the first cycle, 15 mL of the 6PPD-q working solution was mixed with 15 mg of SBAC and agitated for 30 min. After filtration, 12 mL of the filtrate was transferred to another tube containing fresh SBAC to maintain the same solid-to-liquid ratio. This stepwise procedure was repeated, and the 6PPD-q concentrations were measured after each cycle until the guideline value was achieved.

2.4 Fourier-transform infrared spectroscopy

Surface functional groups of SBAC before and after 6PPD-q adsorption were characterised using Fourier-transform infrared spectroscopy (FTIR; Thermo Scientific Nicolet iS50 FTIR Spectrometer, USA). Spectra were obtained in the wavenumber range of 400–4000 cm^{-1} at a resolution of 4 cm^{-1}, averaging 256 scans per sample. Background corrections were applied automatically prior to the analysis.

2.5 Quality control, quality assurance and data analysis

SBAC was prepared by the Geo-Environmental Group at UBC in batches. Each batch was tested for performance consistency using methylene blue as a proxy chemical, and only batches achieving >98% methylene blue removal were blended to form the bulk SBAC used in all experimental tests. To ensure quality, the bulk sample was also tested using the proxy chemical and per- and polyfluoroalkyl substances that had previously undergone over 100 tests.

Fresh 6PPD-q working solutions were prepared before each test and verified using LC–MS/MS analysis. All glassware were pre-cleaned with methanol and thoroughly rinsed with DI water. LC–MS/MS calibration was performed using multi-point curves of 6PPD-q with D5-6PPD-q as the internal standard, with routine checks to ensure consistent performance. Reference solutions were analysed to verify initial concentrations, and controls without SBAC were tested to account for non-adsorptive losses. All adsorption experiments were conducted in triplicate. Statistical analyses were conducted to evaluate differences between experimental conditions, with significance assessed at the 95% confidence level ($p < 0.05$).

3. Results and Discussion

3.1 Surface functional groups of SBAC

The FTIR spectrum of SBAC revealed several distinct absorption bands indicative of its surface chemistry (Fig. 1). The broad signal between 2250 and 3500 cm^{-1} corresponds to O–H stretching vibrations, characteristic of hydroxyl, carboxylic and phenolic groups involved in hydrogen bonding. The band at ~1560 cm^{-1} is attributed to C=O stretching in carboxylic and lactonic groups, consistent with the acidic nature determined by Boehm titration (Table S1) (Nicomel et al., 2022b). The peak near 1030 cm^{-1} reflects C–O stretching in alcohols and ethers, while those between 410 and 800 cm^{-1} are ascribed to aromatic C–H bending vibrations (Hu et al., 2018; Huo et al., 2020). Overall, the presence of these oxygen-containing groups suggests that $ZnCl_2$ activation and subsequent pyrolysis enriched SBAC with surface functionalities favourable for 6PPD-q adsorption through hydrogen bonding and π–π interactions.

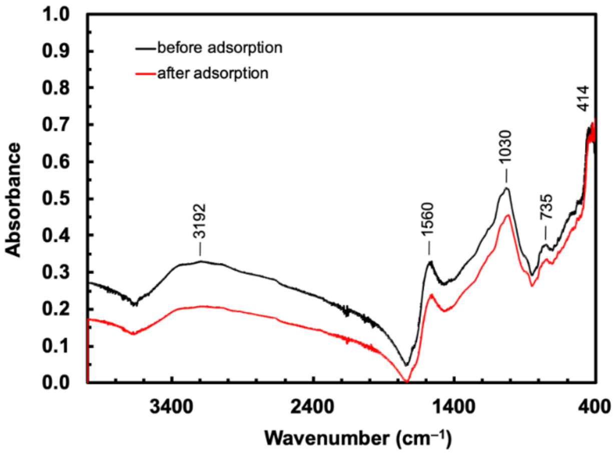

Fig. 1. Fourier-transform infrared spectra of sewage-sludge-based activated carbon before and after 6PPD-quinone (6PPD-q) adsorption, showing absorption bands at 3192 cm^{-1} (O–H stretching), ~1560 cm^{-1} (C=O stretching), 1030 cm^{-1} (C–O stretching) and 410–800 cm^{-1} (aromatic C–H bending vibrations).

3.2 Adsorption capacity

The adsorption capacity of SBAC increased from 14.8 to 499.8 µg/g as the initial concentration of 6PPD-q increased from 20 to 500 µg/L (Fig. 2), indicating that higher contaminant levels enhanced the mass-transfer driving force towards the adsorbent surface (Mangrulkar et al., 2008). At low concentrations, many adsorption sites remained unoccupied, whereas at higher concentrations, more 6PPD-q molecules interacted with the available active sites until surface saturation. Similar trends have been reported previously (Chenchu and Deo, 2025; Gkika et al., 2025), where increased pollutant concentration resulted in enhanced adsorption capacity as the larger concentration gradient facilitated diffusion to active sites. However, the rate of increase gradually diminished at higher concentrations, suggesting that the adsorption process was approaching equilibrium and that the available sites on SBAC were becoming fully occupied. Therefore, an initial concentration of 200 µg/L was selected for the subsequent adsorption experiments.

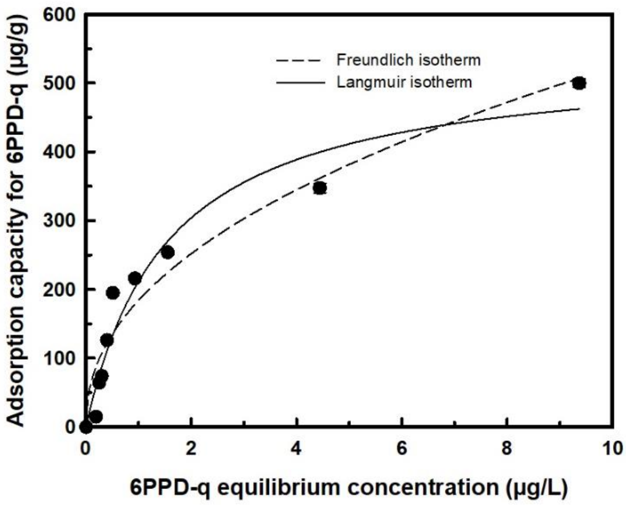

Fig. 2. Adsorption capacity of sewage sludge-based activated carbon (SBAC) towards 6PPD-q at various equilibrium concentrations, with data fitted to Langmuir and Freundlich isotherm models. Experimental conditions: 1 g/L SBAC-to-solution ratio, pH 3.5, 20°C ± 2°C and 0.5 h contact time.

Table 1. Langmuir and Freundlich model parameters for 6PPD-quinone adsorption onto sewage-sludge-based activated carbon (SBAC). Experimental conditions: 1 g/L SBAC-to-solution ratio, 20°C ± 2°C, pH 3.6–3.8 and 0.5 h contact time.

	Langmuir model			Freundlich model		
	q_{max} (µg/g)	b	R^2	K_f (µg$^{1-1/n}$L$^{1/n}$/g)	$1/n$	R^2
SBAC	538.3	0.65	0.95	184.2	0.45	0.94

q_{max} is the maximum adsorption capacity (µg/g), b is the Langmuir adsorption equilibrium constant (L/µg), K_f is the Freundlich constant (µg$^{1-1/n}$ L$^{1/n}$/g) and 1/n is a dimensionless parameter.

Fig. 2 shows the fit of the Langmuir and Freundlich isotherm models to the experimental adsorption data for 6PPD-q at a contact time of 0.5 h. The Langmuir model provided a better fit to the data (Table 1), suggesting that

6PPD-q formed a homogeneous monolayer on the SBAC surface. This observation is consistent with the Langmuir model's assumption of uniform adsorption sites and monolayer coverage (Mende et al., 2018). The estimated q_{max} at 0.5 h suggests that SBAC can achieve near-equilibrium adsorption of 6PPD-q within a short period, indicating rapid adsorption under the tested conditions.

The q_{max} value of SBAC for 6PPD-q was estimated to be 538.3 µg/g using the Langmuir isotherm, highlighting the ability of SBAC to effectively capture this tyre-derived contaminant even at trace concentrations. Although this value is lower than those reported for engineered adsorbents targeting high-concentration pollutants, such as 3D bimetallic nanosheet materials (213.3–335.0 mg/g; Wu et al., 2025), it is sufficient to substantially reduce environmentally relevant levels of 6PPD-q in stormwater. The rapid adsorption observed within 0.5 h suggests that most available sites on SBAC are readily accessible, enabling efficient removal within short contact times. Overall, the combination of moderate q_{max}, fast kinetics and low-cost production positions SBAC as a promising candidate for remediating 6PPD-q pollution in urban runoff, particularly in applications where stringent water-quality guidelines must be satisfied.

3.3 Effect pf adsorbent dosage

The adsorption of 6PPD-q onto SBAC was evaluated at dosages of 1, 2 and 3 g/L using an initial concentration of 200 µg/L and a contact time of 0.5 h (Fig. 3). All dosages achieved near-complete removal, with efficiencies close to 100% (Fig. 3a). However, in terms of residual concentrations, the treated samples still contained 1.13, 0.6 and 0.5 µg/L of 6PPD-q at dosages of 1, 2 and 3 g/L, respectively. These values remain above the short-term acute water-quality guideline of 0.01 µg/L (Chalifour et al., 2025). The marginal increase in removal efficiency between 2 and 3 g/L suggests that the available adsorption sites were not fully utilised, likely owing to the low solute equilibrium concentration and limited driving force for further adsorption (Mangrulkar et al., 2008). To balance material efficiency and treatment performance, the SBAC dosage of 1 g/L was selected for subsequent experiments.

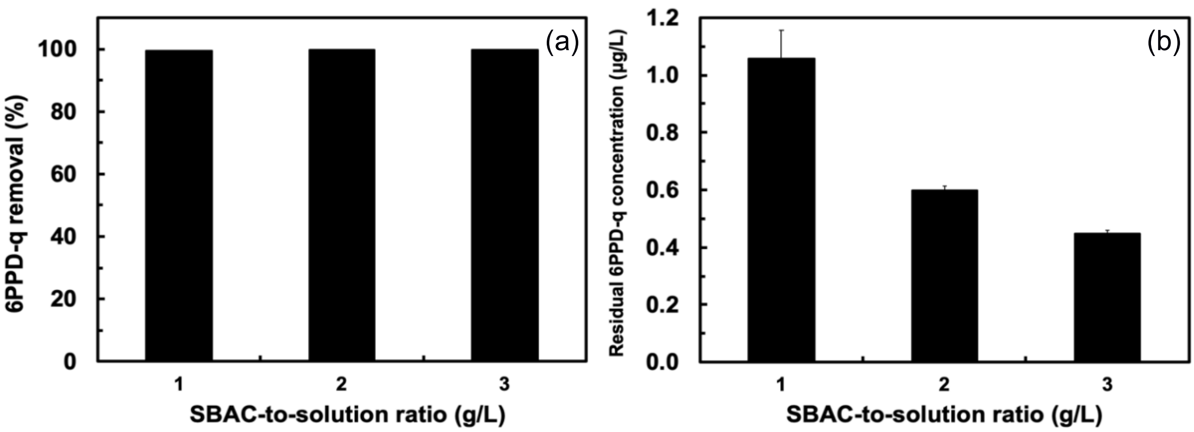

Fig. 3. (a) Removal efficiency and (b) residual concentration of 6PPD-q after adsorption onto SBAC under different SBAC-to-solution ratios. Experiments were conducted at an initial 6PPD-q concentration of 200 µg/L, pH 3.5, 20°C ± 2°C and 24 h contact time. Error bars indicate standard deviations (*n* = 3); where not visible, they fall within the bar boundaries.

3.4 Effect of contact time

The effect of contact time on 6PPD-q removal was evaluated at 0.5 and 24 h (Fig. 4). SBAC achieved nearly complete removal (>99%) under both contact times, whereas the removal efficiency for the control was less than 7%. No significant difference was observed between 0.5 and 24 h for SBAC ($p > 0.05$), indicating that adsorption equilibrium was attained within 0.5 h. This rapid uptake is likely attributable to SBAC's large surface area, abundant surface functional groups and strong affinity of 6PPD-q molecules to the available adsorption sites (Wu et al., 2025). In this scenario, adsorption is potentially driven by π–π interactions or hydrogen bonding with surface functional groups such as carboxylic groups (Correa-Abril et al., 2024). The rapid kinetics demonstrate the effectiveness of SBAC in treating 6PPD-q-contaminated water, providing operational advantages by reducing the required contact time. Based on these results, a contact time of 0.5 h was chosen for subsequent experiments.

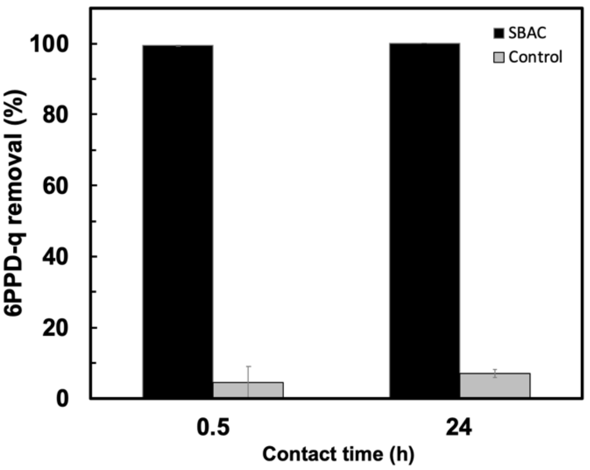

Fig. 4. Removal efficiency of SBAC for 6PPD-q after 0.5 and 24 h adsorption. Experiments were conducted at an initial 6PPD-q concentration of 200 µg/L, pH 3.5, 20°C ± 2°C and 1 g/L SBAC-to-solution ratio. Error bars indicate standard deviations (*n* = 3); where not visible, they fall within the bar boundaries.

3.5 Effect of temperature

Fig. 5 shows the effect of temperature on 6PPD-q removal, evaluated at 7°C, 20°C and 35°C. SBAC achieved almost complete removal (>99%) under all conditions, whereas the control exhibited minimal removal (<6%). The corresponding residual concentrations ranged from 0.65 to 1.06 µg/L. The absence of a clear trend across the tested range indicates that adsorption occurred largely independent of temperature. This behaviour indicates the dominance of strong surface interactions rather than diffusion-controlled mechanisms. Given that adsorption occurred rapidly, temperature changes likely did not affect the transport of 6PPD-q molecules through the surrounding film or into the porous structure of SBAC. This temperature-independent behaviour of SBAC highlights its stability and suitability for stormwater treatment systems (e.g. rain gardens) subject to seasonal or daily temperature variations (Burszta-Adamiak et al., 2023).

The calculated thermodynamic parameters are summarised in Table S2. The negative standard Gibbs free energy change ΔG^0 indicates that the adsorption of 6PPD-q onto SBAC occurs spontaneously under the tested conditions. The positive standard enthalpy change ΔH^0 suggests that the process is endothermic, implying that chemisorption is the dominant mechanism (Wu et al., 2025). Furthermore, the positive standard entropy change ΔS^0 indicates structural modifications in SBAC as well as the strong affinity between 6PPD-q and SBAC (Kusuma et al., 2025).

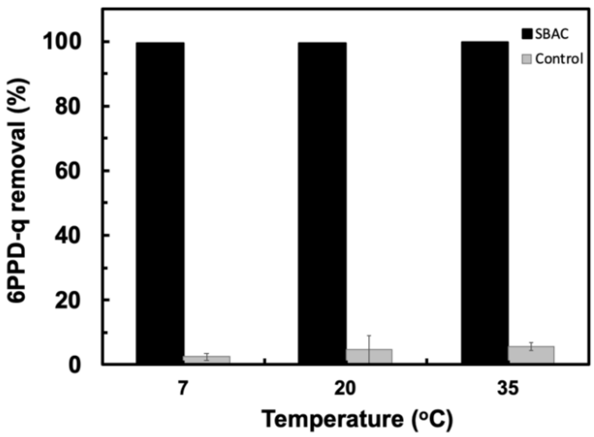

Fig. 5. Removal of 6PPD-q via adsorption onto SBAC for 0.5 h at 1 g/L SBAC-to-solution ratio, pH 3.5 and temperatures of 7°C, 20°C and 35°C ± 2°C. Error bars indicate standard deviations (*n* = 3); where they are not visible, they fall within the bar boundaries.

3.6 Sequential adsorption

The ability of waste-derived SBAC to remove 6PPD-q was evaluated through successive adsorption cycles (Fig. 6). Four sequential runs were performed, each lasting 0.5 h. The first cycle reduced the 6PPD-q concentration from 200 to 1.47 µg/L, and subsequent runs decreased the residual levels to below 0.1 µg/L. Complete removal to below the short-term acute water-quality guideline of (0.01 µg/L; Chalifour et al., 2025) could not be confirmed owing to the LC–MS/MS detection limit of 0.5 µg/L. Nevertheless, the near-complete removal of 6PPD-q after the second run indicates that repeated treatment with fresh SBAC effectively sustains high removal efficiency.

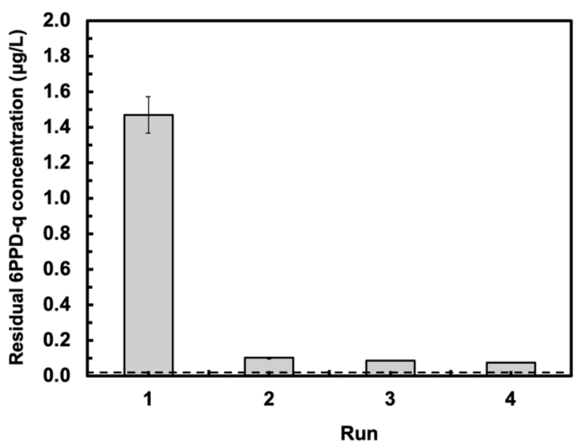

Fig. 6. Residual 6PPD-q concentrations from sequential adsorption tests, with the 0.01 µg/L short-term acute water-quality guideline shown as a dashed line. Experimental conditions: 200 µg/L initial 6PPD-q concentration, 1 g/L SBAC-to-solution ratio, pH 3.5, 0.5 h contact time and 20°C ± 2°C. Error bars indicate standard deviations (*n* = 3); where not visible, they fall within the bar boundaries.

The rapid uptake observed in each 0.5-h run suggests that SBAC performs efficiently even within short contact periods, resulting in lower operating costs in practical applications. These results highlight the potential of SBAC as a cost-effective SS-derived adsorbent, capable of removing tyre-derived contaminants such as 6PPD-q from stormwater. Future work should focus on evaluating adsorption under a wider range of pH values and matrix conditions as well as with enhanced analytical detection limits to better assess removal relative to ecological toxicity thresholds.

4. Conclusion

SBAC demonstrated rapid and efficient removal of 6PPD-q from water, achieving >99% removal from an initial concentration of 200 µg/L within 0.5 h. The adsorption kinetics followed the Langmuir model, with an estimated maximum capacity of 538.3 µg/g, indicating monolayer adsorption on uniform surface sites. These characteristics highlight the suitability of SBAC for integration into stormwater treatment systems, such as rain gardens, bioretention cells and filtration units, where short contact times and variable flow conditions prevail.

The adsorption performance observed for 6PPD-q, along with the physicochemical characteristics of SBAC, indicates potential applicability for removing other organic microcontaminants poorly addressed by conventional treatment processes such as chlorination, ozonation and UV irradiation. However, targeted studies are required to evaluate SBAC performance across different contaminant classes. From a practical perspective, the use of SBAC may help mitigate the cost limitations associated with activated-carbon-based adsorption technologies. The use of SBAC as a waste-derived, low-cost adsorbent aligns with circular economy principles, enabling the conversion of waste SS into a value-added material for mitigating tyre-derived contaminants.

Notably, although 6PPD-q concentrations were reduced to levels near the aquatic-life guideline (0.01 µg/L), further evaluation under varying pH conditions and complex water matrices is needed to confirm the practical applicability of SBAC. Overall, this work positions SBAC as a sustainable and scalable solution for protecting urban waterways from emerging contaminants.

Acknowledgements

The authors thank Brad Wishart for assisting with the LC–MS/MS analysis.

Funding

This work was supported by Mitacs Canada [grant number IT29928].

Author Contributions

Nina Ricci Nicomel: Conceptualisation; Data curation; Formal analysis; Investigation; Methodology; Validation; Visualisation; Writing – Original Draft.

Loretta Y. Li: Conceptualisation; Methodology; Investigation; Formal analysis; Writing – Revising, Editing and proofreading, Visualisation, Supervision, Funding acquisition.

Ethical Approval

Not applicable.

Consent to Participate

Not applicable.

Consent to Publish

Not applicable.

Conflict of Interest

There are no conflicts of interest to declare.

Data Availability Statement

The authors declare that the data supporting the findings of this study are provided within the main text and supplementary information. Raw data files in alternative formats are available from the corresponding author upon reasonable request.

References

B.C. Ministry of Water, Land, and Resource Stewardship (2025). 6PPD-quinone Acute Water Quality Guidelines – Freshwater Aquatic Life, Water Quality Guideline Series, WQG-24. Prov. B.C., Victoria B.C.

Beji, A., Deboudt, K., Khardi, S., Muresan, B., Lumière, L. (2021). Determinants of rear-of-wheel and tire-road wear particle emissions by light-duty vehicles using on-road and test track experiments. *Atmospheric Pollution Research*, 12(3), 278–291. https://doi.org/10.1016/j.apr.2020.12.014.

Björklund, K., Li, L. Y. (2017). Adsorption of organic stormwater pollutants onto activated carbon from sewage sludge. *Journal of Environmental Management*, 197, 490–497. https://doi.org/10.1016/j.jenvman.2017.04.011.

Burszta-Adamiak, E., Biniak-Pieróg, M., Dąbek, P. B., Sternik, A. (2023). Rain garden hydrological performance – responses to real rainfall events. *Science of the Total Environment*, 887, 164153. https://doi.org/10.1021/acs.est.1c07376.

Cao, G., Wang, W., Zhang, J., Wu, P., Zhao, X., Yang, Z., Hu, D., Cai, Z. (2022). New evidence of rubber-derived quinones in water, air, and soil. *Environmental Science and Technology*, 56(7), 4142–4150. https://doi.org/10.1016/j.envpol.2021.117811

Chae, E., Jung, U., Choi, S.-S. (2021). Quantification of tire tread wear particles in microparticles produced on the road using oleamide as a novel marker. *Environmental Pollution*, 288, 117811. https://doi.org/10.1016/j.envpol.2021.117811.

Challis, J. K., Popick, H., Prajapati, S., Harder, P., Giesy, J. P., McPhedran, K., Brinkmann, M. (2021). Occurrences of tire rubber-derived contaminants in cold-climate urban runoff. *Environmental Science and Technology Letters*, 8(*11*), 961–967. https://doi.org/10.1021/acs.estlett.1c00682.

Chalifour, A., Schein, A., Johnson-MacKinnon, J., Sinclair, J. (2025). *6PPD-quinone Acute Water Quality Guidelines for Freshwater Aquatic Life*, B.C. Ministry of Water, Land, and Resource Stewardship. Canada. Retrieved from https://coilink.org/20.500.12592/444l51y on 27 Nov 2025. DOI: 20.500.12592/444l51y.

Chenchu, S. D., Deo, M. (2025). CuO-modified chitosan beads: an efficient adsorbent for nitrate ion removal from aqueous solution for industrial applications. *Results in Surfaces and Interfaces*, 20, 100609. https://doi.org/10.1016/j.rsurfi.2025.100609.

Correa-Abril, J., Stahl, U., Cabrera, E. V., Parra, Y. J., Vega, M. A., Taamalli, S., Louis, F., Rodríguez-Díaz, J. M. (2024). Adsorption dynamics of Cd2+(aq) on microwave-synthetized pristine biochar from cocoa pod husk: green, experimental, and DFT approaches. *iScience*, 27(*6*), 109958. https://doi.org/10.1016/j.isci.2024.109958.

Deutsches Institut für Normung. (2008). *Chemical Analysis - Decision Limit, Detection Limit and Determination Limit under Repeatability Conditions - Terms, Methods, Evaluation*. Berlin, Germany: Deutsches Institut für Normung.

Gkika, D. A., Tolkou, A. K., Katsoyiannis, I. A., Kyzas, G. Z. (2025). The adsorption-desorption-regeneration pathway to a circular economy: the role of waste-derived adsorbents on chromium removal. *Separation and Purification Technology*, 368, 132996. https://doi.org/10.1016/j.seppur.2025.132996.

Greer, J.B., Dalsky, E.M., Lane, R.F., Hansen, J.D. (2023). Tire-Derived Transformation Product 6PPD-Quinone Induces Mortality and Transcriptionally Disrupts Vascular Permeability Pathways in Developing Coho Salmon. Environ. Sci. Technol. 57, 10940–10950. https://doi.org/10.1021/acs.est.3c01040.

Halle, L. L., Palmqvist, A., Kampmann, K., Jensen, A., Hansen, T., Khan, F. R. (2021). Tire wear particle and leachate exposures from a pristine and road-worn tire to Hyalella azteca: comparison of chemical content and biological effects. *Aquatic Toxicology*, 232, 105769. https://doi.org/10.1016/j.aquatox.2021.105769.

Hiki, K., Asahina, K., Kato, K., Yamagishi, T., Omagari, R., Iwasaki, Y., Watanabe, H., Yamamoto, H. (2021). Acute toxicity of a tire rubber-derived chemical, 6PPD quinone, to freshwater fish and crustacean species. *Environmental Science and Technology Letters*, 8(*9*), 779–784. https://doi.org/10.1021/acs.estlett.1c00453.

Hu, J., Danish, M., Lou, Z., Zhou, P., Zhu, N., Yuan, H., Qian, P. (2018). Effectiveness of wind turbine blades waste combined with the sewage sludge for enriched carbon preparation through the co-pyrolysis processes. *Journal of Cleaner Production*, 174, 780–787. https://doi.org/10.1016/j.jclepro.2017.10.166.

Huo, E., Duan, D., Lei, H., Liu, C., Zhang, Y., Wu, J., Zhao, Y., Huang, Z., Qian, M., Zhang, Q., Lin, X., Wang, C., Mateo, W., Villota, E. M., Ruan, R. (2020). Phenols production form Douglas fir catalytic pyrolysis with MgO and biomass-derived activated carbon catalysts. *Energy*, 199, 117459. https://doi.org/10.1016/j.energy.2020.117459.

Jeirani, Z., Niu, C. H., Soltan, J. (2017). Adsorption of emerging pollutants on activated carbon. *Reviews in Chemical Engineering*, 33(*5*), 491–522. https://doi.org/10.1515/revce-2016-0027.

Johannessen, C., Helm, P., Lashuk, B., Yargeau, V., Metcalfe, C. D. (2022). The tire wear compounds 6PPD-quinone and 1,3-diphenylguanidine in an urban watershed. *Archives of Environmental Contamination and Toxicology*, 82(*2*), 171–179. https://doi.org/10.1007/s00244-021-00878-4.

Kusuma, H. S., Jaya, D. E. C., Lantip, G. I. A., Afifah, D. K., Kirani, A. C., Mahfud, M., Darmokoesoemo, H., Amenaghawon, A. N., Kurniawan, T. A. (2025). Theoretical perspectives and recent advances in palm-based adsorbents for sustainable heavy metal removal from aqueous systems. *Desalination and Water Treatment*, 323, 101315. https://doi.org/10.1016/j.dwt.2025.101315.

Lane, R.F., Smalling, K.L., Bradley, P.M., Greer, J.B., Gordon, S.E., Hansen, J.D., Kolpin, D.W., Spanjer, S.R., Masoner, J.R. (2024). Tire-derived contaminants 6PPD and 6PPD-Q: Analyssi, sample handling, and reconnaissance of United States stream exposure. *Chemosphere*, 363, 142830. https://doi.org/10.1016/j.chemosphere.2024.142830.

Li, L. Y., Gong, X., Abida, O. (2019). Waste-to-resources: exploratory surface modification of sludge-based activated carbon by nitric acid for heavy metal adsorption. *Waste Management*, 87, 375–386. https://doi.org/10.1016/j.wasman.2019.02.019.

Liu, Y., Chen, H., Gao, J., Li, Y., Dave, K., Chen, J., Federici, M., Perricone, G. (2021). Comparative analysis of non-exhaust airborne particles from electric and internal combustion engine vehicles. *Journal of Hazardous Materials*, 420, 126626. https://doi.org/10.1016/j.jhazmat.2021.126626.

Luján-Facundo, M. J., Iborra-Clar, M. I., Mendoza-Roca, J. A., Alcaina-Miranda, M. I., Maciá, A. M., Lardín, C., Pastor, L., Claros, J. (2020). Preparation of sewage sludge–based activated carbon for hydrogen sulphide removal. *Water, Air, and Soil Pollution*, 231(*4*), 187. https://doi.org/10.1007/s11270-020-04518-w.

Mangrulkar, P. A., Kamble, S. P., Meshram, J., Rayalu, S. S. (2008). Adsorption of phenol and o-chlorophenol by mesoporous MCM-41. *Journal of Hazardous Materials*, 160(*2–3*), 414–421. https://doi.org/10.1016/j.jhazmat.2008.03.013.

McIntyre, J. K., Prat, J., Cameron, J., Wetzel, J., Mudrock, E., Peter, K. T., Tian, Z., Mackenzie, C., Lundin, J., Stark, J. D., King, K., Davis, J. W., Kolodziej, E. P., Scholz, N. L. (2021). Treading water: tire wear particle leachate recreates an urban runoff mortality syndrome in coho but not chum salmon. *Environmental Science and Technology*, 55(*17*), 11767–11774. https://doi.org/10.1021/acs.est.1c03569.

Mende, M., Schwarz, D., Steinbach, C., Boldt, R., Schwarz, S. (2018). The influence of salt anions on heavy metal ion adsorption on the example of nickel. *Materials*, 11(*3*), 373. https://doi.org/10.3390/ma11030373.

Mohamed, B.A.; Li, L.Y., Hamid, H., Jeronimo, M. (2022). Sludge-based activated carbon and its application in the removal of perfluoroalkyl substances: a feasible approach towards a circular economy. *Chemosphere* 294, 133707. https://doi.org/10.1016/j.chemosphere.2022.133707.

Mohamed, B.A.; Nicomel, N.R., Hamid, H., Li, L.Y. (2023). Using circular economy principles in the optimisation of sludge-based activated carbon production for the removal of perfluoroalkyl substances. *Science of the Total Environment*. 874, 162392. https://doi.org/10.1016/j.scitotenv.2023.162392.

Mohamed, B.A., Hamid, H., Montoya-Bautista, C.V., Li, L.Y. (2023). Circular economy in wastewater treatment plants: Treatment of contaminants of emerging concerns (CECs) in effluent using sludge-based activated carbon. *Journal of Cleaner Production* 389, 136095. https://doi.org/10.1016/j.jclepro.2023.136095.

Montoya-Bautista, C. V., Mohamed, B. A., Li, L. Y. (2022). Sludge-based activated carbon from two municipal sewage sludge precursors for improved secondary wastewater-treatment discharge-effluent. *Journal of Environmental Chemical Engineering*, 10(*6*), 108704. https://doi.org/10.1016/j.jece.2022.108704.

Mu'azu, N. D., Jarrah, N., Zubair, M., Alagha, O. (2017). Removal of phenolic compounds from water using sewage sludge-based activated carbon adsorption: a review. *International Journal of Environmental Research and Public Health*, 14(*10*), 1094. https://doi.org/10.3390/ijerph14101094.

Nicomel, N. R., Li, L. Y., Du Laing, G. (2022a). Biosolids-based activated carbon for enhanced copper removal from citric-acid-rich aqueous media. *Environmental Science and Pollution Research International*, 29(*49*), 74742–74755. https://doi.org/10.1007/s11356-022-21020-4.

Nicomel, N. R., Li, L. Y., Mohamed, B. A., Ramim, S. S. (2022b). Adsorption of p-benzoquinone at low concentrations from aqueous media using biosolid-based activated carbon. *Journal of Environmental Management*, 316, 115263. https://doi.org/10.1016/j.jenvman.2022.115263.

Nicomel, N.R., Li, L. (2023). Review of 6PPD-quinone environmental occurrence, fate, and toxicity in stormwater. Ecocycles 9, 33–46. https://doi.org/10.19040/ecocycles.v9i3.347.

Seiwert, B., Nihemaiti, M., Troussier, M., Weyrauch, S., Reemtsma, T. (2022). Abiotic oxidative transformation of 6-PPD and 6-PPD quinone from tires and occurrence of their products in snow from urban roads and in municipal wastewater. *Water Research*, 212, 118122. https://doi.org/10.1016/j.watres.2022.118122.

Sullivan, G. L., Prigmore, R. M., Knight, P., Godfrey, A. R. (2019). Activated carbon biochar from municipal waste as a sorptive agent for the removal of polyaromatic hydrocarbons (PAHs), phenols and petroleum based compounds in contaminated liquids. *Journal of Environmental Management*, 251, 109551. https://doi.org/10.1016/j.jenvman.2019.109551.

Tian, Z., Zhao, H., Peter, K. T., Gonzalez, M., Wetzel, J., Wu, C., Hu, X., Prat, J., Mudrock, E., Hettinger, R., Cortina, A. E., Biswas, R. G., Kock, F. V. C., Soong, R., Jenne, A., Du, B., Hou, F., He, H., Lundeen, R., Gilbreath, A., Sutton, R., Scholz, N. L., Davis, J. W., Dodd, M. C., Simpson, A., McIntyre, J. K., Kolodziej, E. P. (2021). A ubiquitous tire rubber–derived chemical induces acute mortality in coho salmon. *Science*, 371(*6525*), 185–189. https://doi.org/10.1126/science.abd6951.

Varshney, S., Gora, A. H., Siriyappagouder, P., Kiron, V., Olsvik, P. A. (2022). Toxicological effects of 6PPD and 6PPD quinone in zebrafish larvae. *Journal of Hazardous Materials*, 424(*C*), 127623. https://doi.org/10.1016/j.jhazmat.2021.127623.

Wang, S., Ma, Y., Zhang, X., Shen, Z. (2022). Transport and sources of nitrogen in stormwater runoff at the urban catchment scale. *Science of the Total Environment*, 806(*1*), 150281. https://doi.org/10.1016/j.scitotenv.2021.150281.

Werle, S., Sobek, S. (2019). Gasification of sewage sludge within a circular economy perspective: a Polish case study. *Environmental Science and Pollution Research International*, 26(*35*), 35422–35432. https://doi.org/10.1007/s11356-019-05897-2.

Wu, N., Wang, J., Zheng, B., Liu, Z., Zhao, H., Di, S., Wang, Z., Wang, X., Qi, P. (2025). Insights into the adsorption performance and mechanism of novel 3D bimetallic MOF nanosheets for the high-efficient removal of 6PPD and 6PPD-quinone. *Separation and Purification Technology*, 354, 128904. https://doi.org/10.1016/j.seppur.2024.128904.

Yu, H., Luo, L., Wu, B., He, J., Wang, H., Chen, R., Ji, M., Yang, Q., Zeng, G., Wu, W., Sun, D. (2025). Efficient catalytic degradation and detoxification of 6PPD-quinone by the multifunctional enzyme system of Phanerochaete chrysosporium. *Journal of Hazardous Materials*, 494, 138634. https://doi.org/10.1016/j.jhazmat.2025.138634.

Yu, W., Tang, S., Wong, J. W. C., Luo, Z., Li, Z., Thai, P. K., Zhu, M., Yin, H., Niu, J. (2024). Degradation and detoxification of 6PPD-quinone in water by ultraviolet-activated peroxymonosulfate: mechanisms, byproducts, and impact on sediment microbial community. *Water Research*, 263, 122210. https://doi.org/10.1016/j.watres.2024.122210.

Yue, C., Li, L. Y., Johnston, C. (2018). Exploratory study on modification of sludge-based activated carbon for nutrient removal from stormwater runoff. *Journal of Environmental Management*, 226, 37–45. https://doi.org/10.1016/j.jenvman.2018.07.089.

Zhao, H., Zhong, H., Jiang, Y., Li, H., Tang, P., Li, D., Feng, Y. (2022). Porous ZnCl2-activated carbon from shaddock peel: methylene blue adsorption behavior. *Materials*, 15(*3*), 895. https://doi.org/10.3390/ma15030895.

Supplementary Information (SI)

Section S1. Data analysis

The removal efficiencies and adsorption capacities of SBAC for 6PPD-q were calculated using Equations 1 and 2, respectively.

$$R\,(\%) = \frac{C_0 - C_e}{C_0} \times 100 \quad (1)$$

$$q = \frac{(C_0 - C_e) \times V}{m} \quad (2)$$

Where R is the removal efficiency (%), q is the amount of 6PPD-q adsorbed per unit mass of SBAC (μg/g), C_0 and C_e are the initial and equilibrium 6PPD-q concentrations (μg/L), respectively, V is the volume of the 6PPD-q solution (L), and m is the mass of SBAC (g).

Langmuir (Equation 3) and Freundlich (Equation 4) adsorption isotherm models were used to fit the experimental adsorption data at different initial 6PPD-q concentrations. SigmaPlot Version 11.0 was used to determine the adsorption isotherms and the corresponding parameters.

$$q_e = \frac{q_{max} b C_e}{1 + bC_e} \quad (3)$$

$$q_e = K_f {C_e}^{1/n} \quad (4)$$

Where q_e is the amount of 6PPD-q adsorbed per unit mass of SBAC at equilibrium (μg/g), q_{max} is the maximum adsorption capacity (μg/g), b is the Langmuir adsorption equilibrium constant (L/μg), C_e is the equilibrium 6PPD-q concentration (μg/L), K_f is the Freundlich constant ($\mu g^{1-1/n}\,L^{1/n}/g$) and 1/n is a dimensionless parameter.

Section S2. Data analysis

The thermodynamics parameters, such as Gibbs free energy ΔG^0 (kJ mol^{-1}), standard enthalpy change ΔH^0 (kJ mol^{-1}) and standard entropy change ΔS^0 (kJ $mol^{-1}K^{-1}$), were calculated according to Eqs. 5 and 6.

$$\Delta G^0 = -RT \ln K_0 \quad (5)$$

$$\ln K_0 = -\frac{\Delta H^0}{RT} + \frac{\Delta S^0}{R} \quad (6)$$

Where K_0 is the ratio of equilibrium adsorption capacity (q_e) of SBAC for 6PPD-q to the equilibrium 6PPD-q concentration (C_e); R is the universal gas constant (8.314×10^{-3} kJ $mol^{-1}K^{-1}$); T (K) is the absolute temperature. The relationship between $\ln K_0$ and 1/T was drawn and ΔH^0 and ΔS^0 are equal to the slope and intercept, respectively, in Fig. S1.

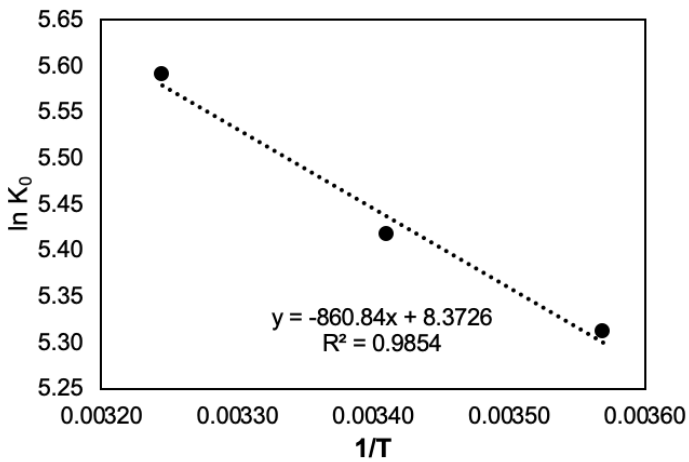

Fig. S1. Plot of $\ln K_0$ versus $1/T$ for the estimation of thermodynamic parameters of 6PPD-q adsorption onto sewage sludge-based activated carbon (SBAC). Experimental conditions: 1 g/L SBAC-to-solution ratio, 200 μg/L, pH 3.6–3.8, and 0.5 h contact time.

Table S1. Physical and chemical characteristics of the sludge-based activated carbon (SBAC).

Parameter	**Value**
Total carbon (%)	60.0
Total nitrogen (%)	5.67
BET-SSA (m^2/g)	723
TPV (cm^3/g)	0.266
CEC (meq/100 g)	1.41
pH (in $CaCl_2$)	2.81
IEP	5.07
PZC	5.80
Carboxylic groups (mmol/g)	0.58
Lactonic groups (mmol/g)	28
Phenolic groups (mmol/g)	0
Total acidic sites (mmol/g)	28.6
Particle size (μm)	d_{10}: 16.8
	d_{50} 76.2
	d_{90}: 180.5

IEP – isoelectric point;
PZC – point of zero charge;
CEC – cation exchange capacity;
BET-SSA – Brunauer-Emmet-Teller specific surface area;
TPV – total pore volume
d_{10} – particle size diameter of 10% of the volume distribution
d_{50} – particle size diameter of 50% of the volume distribution (volume median diameter)
d_{90} – particle size diameter of 90% of the volume distribution

Table S2. Thermodynamic parameters for the adsorption of 6PPD-q onto sewage sludge-based activated carbon (SBAC). Experimental conditions: 1 g/L SBAC-to-solution ratio, 200 µg/L, pH 3.6–3.8, and 0.5 h contact time.

Adsorbent	Temperature (K)	ΔG^0 (kJ mol^{-1})	ΔS^0 (kJ mol^{-1} K^{-1})	ΔH^0 (kJ mol^{-1})
	280	-12.37		
SBAC	293	-13.20	0.070	7.16
	308	-14.32		